MICHIGAN STATE UNIVERSITY

CYCLOTRON LABORATORY

STOPPING POWER, EQUILIBRATION, AND COLLECTIVE FLOW OF NUCLEAR MATTER IN THE REACTION Ar (0.8 GeV/N) + Pb-- A THEORETICAL ANALYSIS

JOSEPH J. MOLITORIS and HORST STÖCKER

APRIL 1985

MSUCL-504

MSUCL-504
April 1985

Stopping Power, Equilibration, and Collective Flow of Nuclear Matter in the Reaction Ar (0.8 GeV/N) + Pb -- A Theoretical Analysis

Joseph J. Molitoris and Horst Stöcker

Department of Physics and Astronomy and
National Superconducting Cyclotron Laboratory
Michigan State University, East Lansing, Michigan 48824

Abstract

The approach to local kinetic equilibrium in relativistic heavy ion collisions is studied by following the time evolution of the Wigner function in configuration and momentum space using the Vlasov-Uehling-Uhlenbeck theory. Rapid equilibration of the participant region is observed within time spans on the order of 10 fm/c. Total stopping of the projectile occurs at small impact parameters, the projectile is consumed by the Pb target. Collective sidewards flow of nuclear matter is predicted. The flow angle distributions are peaked at ≈20° for intermediate impact parameters, $b \approx 5$ fm, and are skewed towards 90° for central collisions, $b < 3$ fm. Recent data from the GSI/LBL Streamer Chamber Group for Ar (770 MeV/N) + Pb support our theoretical analysis. Flow of the projectile is also observed via a pronounced peak structure in the rapidity dependence of the transverse momentum transfer. We predict simultaneously the bounce-off effect of the projectile fragments and the sidesplash of the participant matter observed recently for symmetric systems by the GSI/LBL Plastic Ball collaboration. The flow effects in the asymmetric system are less sensitive to the compressibility and to the Pauli principle than in symmetric collisions. The Pauli principle does, however, have a significant effect on the calculated pion yields.

Thermodynamic and statistical concepts such as temperature and pressure, dissipation and fluctuations, condensation and evaporation, and phase transitions have long been used to characterize the properties of excited nuclear matter formed in relativistic heavy ion collisions. However, the point has long been made that such systems must exhibit substantial nonequilibrium features. Recently the collective sidewards flow of nuclear matter has been unambiguously identified in symmetric[1] as well as asymmetric[2] collision systems, in qualitative agreement with the longstanding predictions of the nuclear fluid dynamical model[3] which depend on local thermal equilibrium as a prerequisite.

For symmetric systems and central impact parameters well defined peaks occur in the flow angular distribution.[1] In asymmetric systems one observes a broad momentum flow angle distribution for high multiplicity (small impact parameters) and a distinct sidewards peak for medium multiplicities (intermediate impact parameters). For light symmetric systems ($A_T \approx A_p \leq 40$) flow effects are not observed[4] when the standard kinetic energy flow tensor[5] is used. However, a novel transverse momentum analysis technique does exhibit flow in Ar (1.8 GeV/N) + KCl experimentally[6] and has been shown theoretically to be sensitive to the nuclear matter equation of state.[7]

Spurred by the availability of experimental data for Ar (770 MeV/N) + Pb from the LBL-GSI streamer chamber group,[2] we have studied the stopping and the approach to equilibrium by simulating the time development of Ar + Pb reactions in the Vlasov-Uehling-Uhlenbeck[7-11] approach. The principal theoretical results of this paper, namely the time development of the nucleons' distribution function in configuration and momentum space, are shown in Figs. 1 and 2. The predictions of the present theory on nuclear

stopping and collective flow are confirmed by the experimental data.[2] This is discussed in detail below.

Recall that the Vlasov-Uehling-Uhlenbeck equation[11] is given by

$$\frac{\partial}{\partial t} f + \vec{v} \cdot \frac{\partial}{\partial \vec{r}} f - \nabla U \cdot \frac{\partial}{\partial \vec{p}} f = -\int \frac{d^3p_2 d^3p_1' d^3p_2'}{(2\pi)^6} \sigma v_{12} \times$$
$$[ff_2(1-f_1')(1-f_2') - f_1'f_2'(1-f)(1-f_2)]\delta^3(p+p_2-p_1'-p_2') \quad (1)$$

This equation gives the time evolution of the single particle distribution function f(r,p,t) under the influence of a mean potential field U in a system with two body collisions and the Pauli principle. The equation may be derived from the quantum Liouville equation by introducing the Wigner function and truncating the BBGKY hierarchy; as in the analogous but classical derivation of the Boltzmann equation, one then makes and intelligent stossahlansatz for the collision term based upon the gain and loss of particles in phase space. We actually go beyond this equation in the VUU theory by introducing both particle creation and as much of special relativity as is possible.[8,9] Protons, neutrons, deltas and pions of different isospin are included separately with their experimental scattering cross sections. For the density dependent potential field, $U(\rho)$, a local Skyrme interaction is used with a compressibility coefficient of K=380 MeV: $U(\rho) = -124\ \rho/\rho_o + 70.5\ (\rho/\rho_o)^2$ MeV. This hard equation of state has been found necessary to explain the pion yields[8] and collective flow effects[8] in symmetric collisions within the context of the present model. We also employ a different Skyrme interaction with K=200 MeV to look for effects of the nuclear equation of state.

To understand the physics in this non-equilibrium situation, let us examine the evolution of the single particle distribution function as obtained from the VUU approach for Ar (770 MeV/N) + Pb collisions. In figures 1 and 2 we display projections of the distribution function into configuration and momentum space for this system. (Note that for ease of viewing, we have flipped both the x and z axis in the configuration space plots and also the p_z axis in the momentum space plots.) The collision term is essential at both intermediate and high energies, as one expects intuitively. Note in figures 1 and 2 that at low impact parameter the Ar projectile is completely consumed by the Pb target as well in configuration as in momentum space. The t=0 configuration space plots show the correct nucleon-nucleon center of momentum frame Lorentz length contraction by a factor $1/\gamma = .85$. In configuration space, for t=10 fm/c, the squashed elliptical to octupole shape is an indication of the high density formed in these collisions. For example, at 1 fm impact parameter, the density within a sphere of radius 2 fm centered at the origin reaches 2.7 ρ_o at 5 fm/c time; then, the density falls very rapidly - by 17 fm/c it is below the ground state value. The directed sidewards flow of nucleons is easily seen in configuration space at b = 3 and 5 fm by the excess of nucleons in the quadrant with $x < 0$ and $z < 0$ (as opposed to $x < 0$ and $z > 0$) as early as t=20 fm/c. Spectator fragments are also observed, namely at 5 fm. The projectile is seen to not just shear off the target; it rather experiences a substantial transverse momentum transfer away from the region of high density - the bounce-off effect predicted earlier on the basis of nuclear fluid dynamics.[3] Thus simple geometric models can only be a very rough approximation to the more complicated reaction dynamics illustrated here.

The momentum space evolution of the single particle distribution function displayed in Fig. 2 exhibits rapid equilibration at low impact parameters: observe that the projectile sphere in momentum space is rapidly depopulated by two body collisions at b = 1 and 3 fm. At t = 5 fm/c substantial filling of the nucleon-nucleon center of momentum region is observable, signaling the formation of a participant zone. At t = 10 fm/c, there are practically no nucleons left in the originally densely populated projectile momentum sphere; almost all of the projectile nucleons have been scattered out of their initial momentum states. At b = 1 fm, this scattering has been with about equal probability into the positive and negative p_x direction. At b = 3 fm, a preference for the positive p_x direction can clearly be observed - this is due to the expansion of the compressed participant matter away from the high density repulsive interaction into the vacuum. At t = 40 fm/c the number of hard nucleon - nucleon collisions has become negligible, the final state in momentum space is closely approached. Observe that secondary, tertiary, etc. collisions of the participants with the target spectator have resulted in a further decrease of the number of fast particles and in a more diffuse momentum distribution in the projectilehemisphere, with a very pronounced sidewards flow visible at b = 3 fm.

At the intermediate impact parameter, b = 5 fm, the situation is even more complicated: since projectile and target exhibit only about half overlap, there are a substantial number of projectile nucleons which do not experience collisions with the target nucleons. Hence the depopulation of the projectile momentum sphere is incomplete, part of the projectile is stopped and forms the participant zone together with the struck nucleons from the target, while the projectile spectators move ahead with nearly

their initial longitudinal momentum. The behavior of the participant nucleons is nearly the same as at the lower impact parameters - equilibration is achieved rapidly (t = 10 fm/c) and sidewards flow is observed. The projectile nucleons which have not undergone collisions, and thus the projectile like fragments formed from them, exhibit a finite transverse momentum transfer into the same direction as the directed participant side splash. This bounce-off[3] of the participants is a result of the repulsive interactions felt by the spectators in the vicinity of the compression zone. The simultaneous occurrence of this bounce off and the sidesplash has recently been experimentally observed[1] in symmetric systems with high statistical confidence. A theoretical analysis of these processes for symmetric systems is presently underway.[10]

The equilibration at low impact parameter goes hand in hand with nuclear stopping; without the collision term, the nuclei are transparent. As a reference case, we have also solved the Vlasov equation by turning off the collision term; then the final momentum distribution looks very much like the initial one, as is the case also at lower energies.[9] An easily accessible experimental quantity is the longitudinal momentum p_z in the laboratory frame. The multiplicity dependence of this quantity should give information on the nuclear stopping. We show in Fig. 3 the longitudinal momentum spectrum at b= 1 fm and 5 fm in the final state. Note that initially the Ar nuclei form a bump at beam momentum p_z= 1430 MeV/c whereas the Pb nuclei are at rest. In the final state at the lower impact parameter we see evidence of nuclear stopping: there is no projectile remnant and the Pb target is accelerated. At the higher impact parameter, there is less stopping: one sees some projectile remnants and the target-like fragments are accelerated less.

One sees from Fig. 2 that in order to detect the collective sidewards flow of nuclear matter one needs to look at the projectile hemisphere $p_z < 0$ in momentum space. An asymmetry here is evidence of collective flow; this is easily observed at the intermediate impact parameter b = 5 fm in Fig. 2. Observe that the flow of nucleons in momentum space is correlated with a flow in configuration space, as is the case also for symmetric systems.[7,8]

Let us compare the predictions of the VUU approach to the data of the GSI-LBL streamer chamber group[2]. The experimentalists analyzed their data using the momentum flow tensor:

$$P_{ij}=\Sigma_\nu[p_i(\nu)p_j(\nu)/\mathrm{abs}(p(\nu))]/\Sigma_\nu \mathrm{abs}(p(\nu)) \quad (2)$$

The data analysis proceeds on an event by event basis in a rather non-trivial way. First, only charged particles are used. Then the center of mass velocity for each event is computed from the momenta of all charged particles with transverse momenta per nucleon greater than the Fermi momentum. Then only the forward hemisphere of this participant center of mass frame is analyzed. Their results are shown in Fig. 4a. We compare in Fig. 4b the corresponding predictions of the Vlasov-Uehling-Uhlenbeck theory. Both in theory and experiment a broad bump is observed in the angular distribution of flow angles for near central collisions, while a rather sharp peak occurs at 15-30 degrees for the medium impact parameters, i.e. intermediate multiplicity events. This contrasts strongly with the results of intranuclear cascade calculations,[12,13] which exhibit forward peaked angular distributions independent of impact parameter as well for asymmetric[2] as for symmetric collisions.[1,3,8,12,13]

We have also done the flow analysis in the more rigidly defined nucleon-nucleon center of momentum system with the coalescence invariant kinetic energy flow tensor[5]:

$$K_{ij} = \Sigma_\nu p_i(\nu) p_j(\nu)/2m(\nu) \quad (3)$$

The analysis is also restricted to the projectile momentum hemisphere $p_z < 0$ since this will avoid the distortion of the event shape by the large number of target spectators at rather small momenta and thus best reflect the flow of the participant nucleons. We see in Fig. 4c that the flow distribution changes it's characteristics in particular for the high multiplicity events. One now sees a distribution skewed towards 90° for the small impact parameters, while the peak remains near 20° degrees for the intermediate impact parameters. This is similar to the results for symmetric systems; the peak of the flow angle distribution decreases with increasing impact parameter[1,3,8,10,14].

In figure 5 we compare the standard kinetic energy flow distributions for individual impact parameters to the novel transverse momentum analysis of Danielewicz and Odyniec[6] that provides a sensitive test for collective flow and it's dependence on the nuclear equation of state in light systems.[7] We analyze the transverse momentum spectrum $p_x(y)$ where

$$y = 1/2 \ln (E+p_{par})/(E-p_{par}) \quad (4)$$

is the rapidity, E is the total energy of the fragment, and p_{par} is the momentum in the beam z-direction. Note that in our simulations, the projectile has $p_{par} = p_z > 0$; in the configuration and momentum space plots,

we have simply flipped the axis for ease of viewing. This technique has also been used to predict the presence of collective flow for ^{16}O (600 MeV/A) + ^{16}O within a time dependent Dirac equation approach.[15]

As is evident from Fig. 2, the flow angle approaches it's asymptotic value rather rapidly; indeed at b= 3 fm, the final flow angle distribution is established in less than 20 fm/c. At b = 1 fm, the flow angle distribution is skewed to 90 degrees, i.e., the projectile momentum hemisphere exhibits sidewards peaking as is evident from Fig. 2; a significant number of particles are thrust to the side perpendicular to the beam axis. A broad peak around 55 degrees is observed at b = 3 fm; the flow angle begins to become well defined. For b = 5 fm, there is a clear peak at 20-30 degrees. Thus it is only at the intermediate impact parameters that the flow is evident by a sharp peak in such asymmetric systems. Part of the reason why the peak is not so pronounced at lower impact parameters is statistical: the projectile hemisphere contains substantially fewer fragments in the final state in an Ar + Pb collision than in a Nb + Nb collision.

In the transverse momentum plots, much the same behavior is seen. However, here the analysis is not restricted to the forward hemisphere in momentum space. Summation over p_x and division by the number of protons in each rapidity bin shows very little flow effects in the target rapidity region, which is dominated by target spectator matter. At b = 1 fm, p_x/N is about 50 MeV/c/N at projectile rapidity, y_p = 0.60, whereas at target rapidity, y_T = -.60, p_x amounts to only 25 MeV/c/N. The flow at b = 3 fm is particularly pronounced in this method of analysis: $p_x(y_p)$ = 150 MeV/c/N whereas $p_x(y_T)$ = 40 MeV/c/N. At b = 5 fm, we have much the same result as at b = 3 fm. Note that in the massive system studied here the transverse

momentum transfer (bounce-off effect[3]) is larger than in lighter systems at higher energies - 100 MeV/c/N have been observed for the system Ar (1.8 GeV/N) + KCl.[6]

We have also looked for effects of the nuclear equation of state by varying the compressibility from K=380 MeV to K=200 MeV at b=1,3 and 5 fm. At the lower impact parameter, the broad distribution prevents any statistically significant difference from being seen. At the intermediate impact parameter, we see a small shifting of the flow angle peak to the smaller angles as the compressibility decreases; this is consistent with but less dramatic than what we have found for symmetric systems.[8,10] Note that one sees a great difference if K=0 MeV, i.e., the cascade model is used; then the distributions are peaked at zero degrees for all impact parameters.[2] An equation of state with compressional energy seems essential to qualitatively reproduce the data; but asymmetric systems appear to be less sensitive to the details of the equation of state than symmetric collisions.[8,10] Furthermore, we have looked for quantal effects by turning off the Pauli principle at b= 3 and 5 fm. No strong effects are seen. This is somewhat of a surprise in view of the strong effect we see in the symmetric case[8,10] and the fact that about 50% of the collisions are Pauli blocked even at this high energy. However, this may perhaps be understood by the fact that many of the blocked collisions are between nucleons in the same nucleus, not between nucleons in the compression zone.

We have also studied the same system at a lower energy 400 MeV/N (see Fig. 5). The kinetic energy flow angle distribution becomes more forward peaked at fixed impact parameter b = 5 fm. The transverse momentum transfer $p_x(y_p)$ decreases to 100 MeV/c/N. The similar system Ar (92 MeV/N) + Au shows what happens in an event by event analysis as the energy is decreased

further: the flow distributions at b= 2, 3, and 4 fm impact parameter become very broad; the transverse momentum at beam and target rapidities is zero to within 10 MeV/c/N. At still lower energies, the transverse momenta spectra are inverted as the attractive part of the nuclear potential becomes dominant:[10] the bounce-off caused by the short range repulsion at high density is converted into the negative angle deflection known from TDHF calculations in this energy region[16] and from experimental data.[17]

What about the pions produced in these asymmetric nucleus-nucleus collisions? The pions are created in nucleon-nucleon collisions according to experimental cross sections. We have observed that the pions tend to escape in the target ($z < 0$ hemisphere in configuration space) at low impact parameter and to the left away from the high density zone at intermediate impact parameter. The total average pion multiplicities vary from 10.6 at b= 1 fm to 3.7 at b= 7 fm. About 26-30% more pions are created when the Pauli principle is turned off. This is understood physically: with the Pauli principle turned off, the final state phase space in the intermediate rapidity region is more strongly occupied; equivalently, with the Pauli principle turned on, many collisions that would otherwise produce pions are forbidden by Pauli blocking. What about the time development of the pion numbers? At b= 1 fm, the pion number rises to a maximum of 12.1 at t= 15 fm/c; pions are then reabsorbed until a stable value of 10.6 is reached at t= 30 fm/c.

In summary, we have studied the asymmetric system Ar + Pb in the Vlasov-Uehling-Uhlenbeck theory. We find evidence of nuclear stopping at low impact parameters and rapid (t = 10 fm/c) equilibration with a participant zone forming at intermediate impact parameters. Collisions from 50 MeV/N to 1000 MeV/N probe different parts of the nuclear potential. We

see that at lower energies, the attractive part of the potential is felt. Around 100 MeV/N, there is a change in polarity in the transverse momentum spectra. Then as the energy is increased further, the repulsive nuclear potential is probed. The compressed nuclear matter pushes projectile remnants away from the beam axis, thus creating the bounce off effect at intermediate impact parameters. The collective sidewards expansion of the compressed nuclear matter is recognized in the sidesplash phenomenon.

References:

1. H.A. Gustafsson, H.H. Gutbrod, B. Kolb, H. Löhner, B. Ludewigt, A. M. Poskanzer, T. Renner, H. Riedesel, H.G. Ritter, A. Warwick, F. Weik, H. Wieman, Phys. Rev. Lett. 52, 1590 (1984).

2. R. E. Renfordt, D. Schall, R. Bock, R. Brockmann, J.W. Harris, A. Sandoval, R. Stock, H. Ströbele, D. Bangert, W. Rauch, G. Odyniec, H.G. Pugh, L.S. Schroeder, Phys. Rev. Lett. 53, 763 (1984).

3. H. Stöcker, J.A. Maruhn, W. Greiner, Phys. Rev. Lett. 44, 725 (1980). G. Buchwald, G. Graebner, J. Theis, J. Maruhn, W. Greiner, H. Stöcker, Phys. Rev. Lett. 52, 1594 (1984); Phys. Rev. C 28, 2349 (1983).

4. H. Ströbele, R. Brockmann, J.W. Harris, F. Riess, A. Sandoval, H.G. Pugh, L.S. Schroeder, P.E. Renfordt, K. Tittel, M. Maier, Phys. Rev. C27, 1349 (1983).
H. Ströbele, Nucl. Instr. and Meth. 221, 523 (1984).

5. M. Gyulassy, K.A. Fraenkel, H. Stöcker, Phys. Lett. 110B (1982) 185.

6. P. Danielewicz and G. Odyniec, LBL-18600 preprint.

7. J.J. Molitoris and H. Stöcker, MSUCL-501, Phys. Rev. C, in print.

8. H. Kruse, B.V. Jacak, H. Stöcker, Phys. Rev. Lett., 54, 289 (1985).

9. H. Kruse, B.V. Jacak, J.J. Molitoris, G.D. Westfall, H. Stöcker, Phys. Rev. C, 31 (1985).

10. J.J. Molitoris and H. Stöcker, MSUCL-514, to be published.

11. E.A. Uehling and G.E. Uhlenbeck, Phys. Rev. 43, 552 (1933).

12. J. Cugnon, D. L'Hote, Phys. Lett. 149B, 35 (1984) and
J.J. Molitoris, H. Stöcker, J. Cugnon, D. L'Hote, to be published.

13. Y. Yariv, Z. Fraenkel, Phys. Rev. C 20, 2227 (1979);
Z. Fraenkel, Nucl. Phys. A428, 373c (1984) and private communication.

14. J.J. Molitoris, J.B. Hoffer, H. Kruse, H. Stöcker, Phys. Rev. Lett. 53, 899 (1984).

15. R.Y. Cusson, P.G. Reinhard, H. Stöcker, M.R. Strayer, W. Greiner, MSUCL-497, Phys. Rev. Lett., in print.

16. H. Stöcker, R.Y. Cusson, J. Maruhn, W. Greiner, Z. Physik A294, 125 (1980); Phys. Lett. 101B, 379 (1981).

17. C.K. Gelbke, N. Trautmann, private communication.

Figure Captions

Fig. 1 The evolution of Ar (770 MeV/N) + Pb in configuration space at:

a) b = 1 fm;

b) b = 3 fm;

c) b = 5 fm.

The results from 30 ensembles are superimposed in order to represent the distribution function.

Fig. 2 The time development of Ar (770 MeV/N) +Pb in momentum space at:

a) b = 1 fm;

b) b = 3 fm;

c) b = 5 fm.

Again, the results from 30 ensembles are superimposed.

Fig. 3 Longitudinal momentum spectra illustrate the stopping power of Ar (770 MeV/N) + Pb reactions at two different impact parameters.

Fig. 4 Two different methods for detecting collective flow are shown:

a) the standard kinetic energy flow analysis in the NN center of momentum frame is done on the forward hemisphere for b = 1,3, and 5 fm.

b) the transverse momentum analysis is shown at the same impact parameters.

Fig. 5 Flow angle distributions for Ar (770 MeV/N) + Pb:

a) the experimental data with high and low multiplicity cuts analyzed using the momentum flow tensor;

b) corresponding predictions of the Vlasov-Uehling-Uhlenbeck theory;

c) a standard kinetic energy flow analysis done in the nucleon-nucleon center of momentum frame using only the projectiie momentum hemisphere.

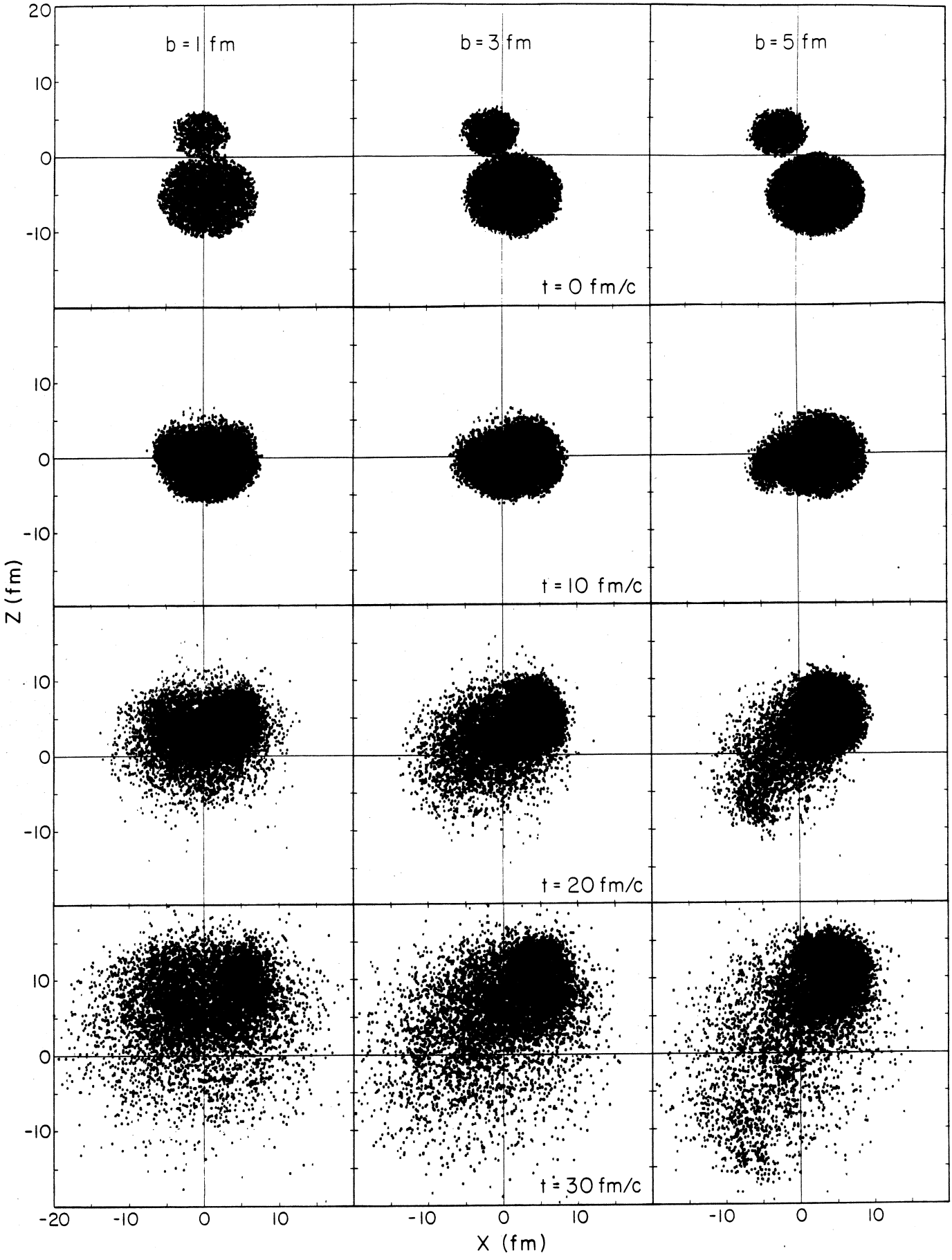
b = 1 fm
b = 3 fm
b = 5 fm
t = 0 fm/c
t = 10 fm/c
t = 20 fm/c
t = 30 fm/c
Z (fm)
X (fm)
20
10
0
-10
-20

FIGURE 1

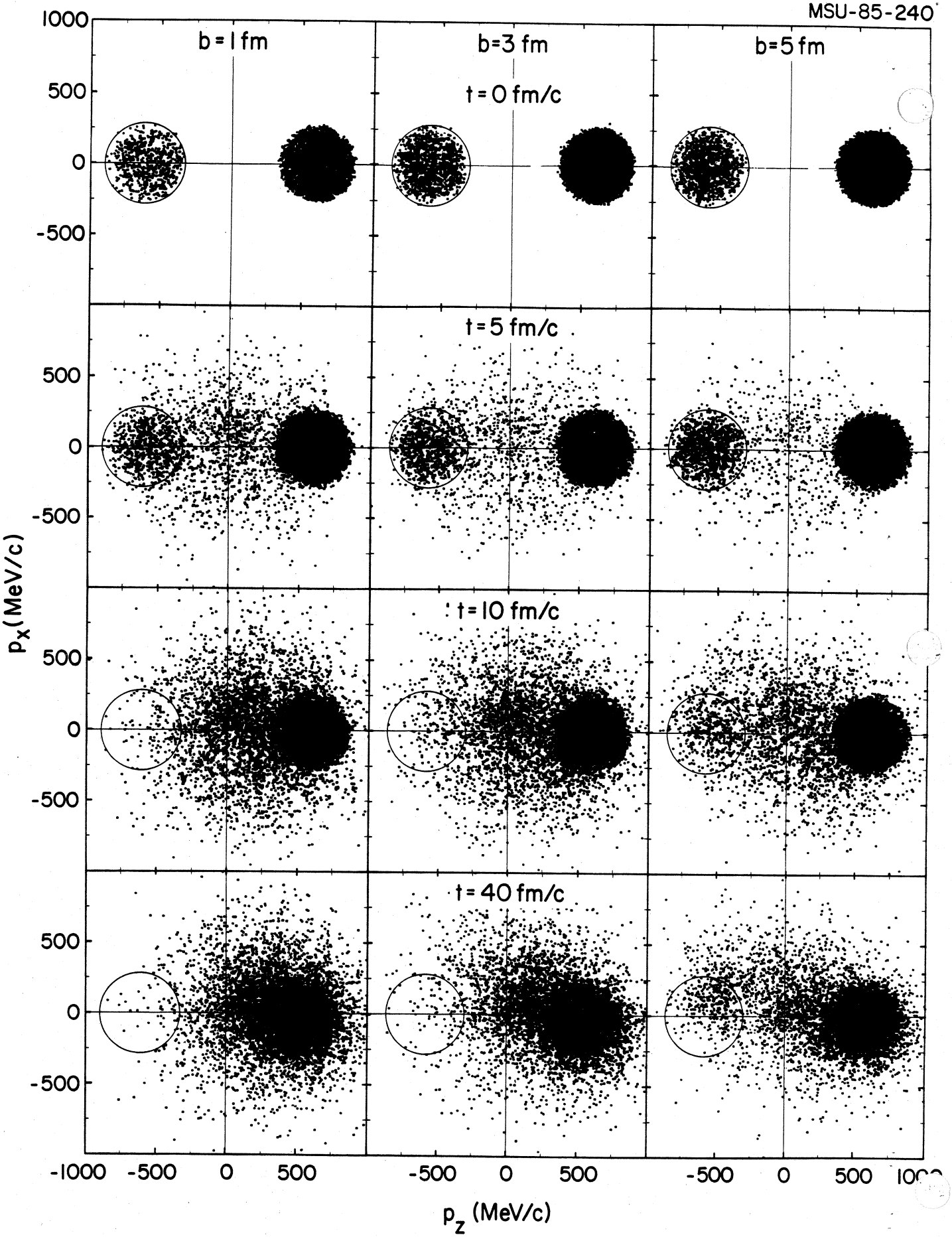
b = 1 fm
b=3 fm
b=5 fm
t = 0 fm/c
t = 5 fm/c
t = 10 fm/c
t = 40 fm/c
1000
500
0
-500
-1000
p_x (MeV/c)
p_z (MeV/c)

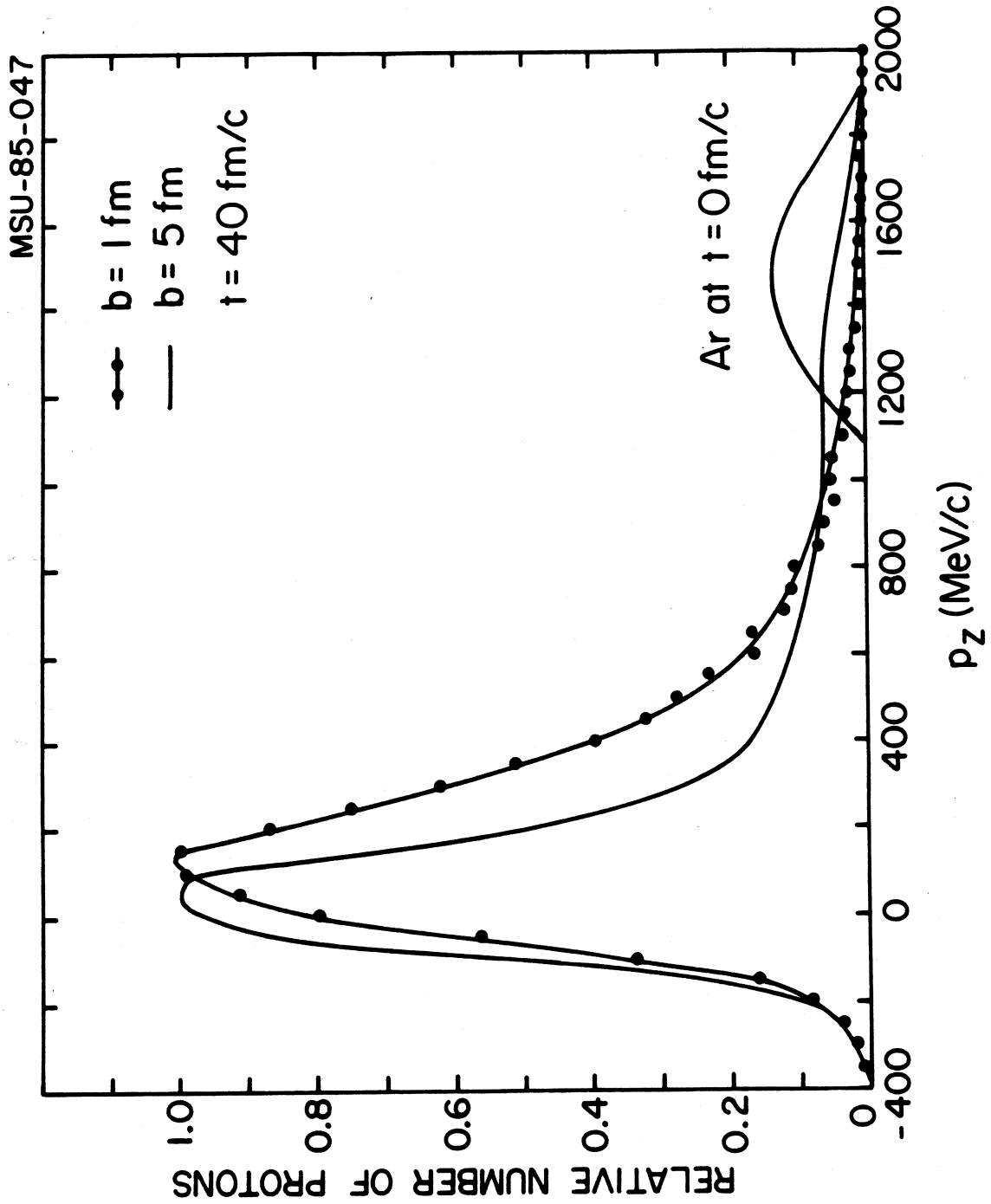
MSU-85-047
b= 1 fm
b= 5 fm
t= 40 fm/c
Ar at t=0 fm/c
RELATIVE NUMBER OF PROTONS
1.0
0.8
0.6
0.4
0.2
0
-400
0
400
800
1200
1600
2000
p_z (MeV/c)

FIGURE 3

MSU-85-046

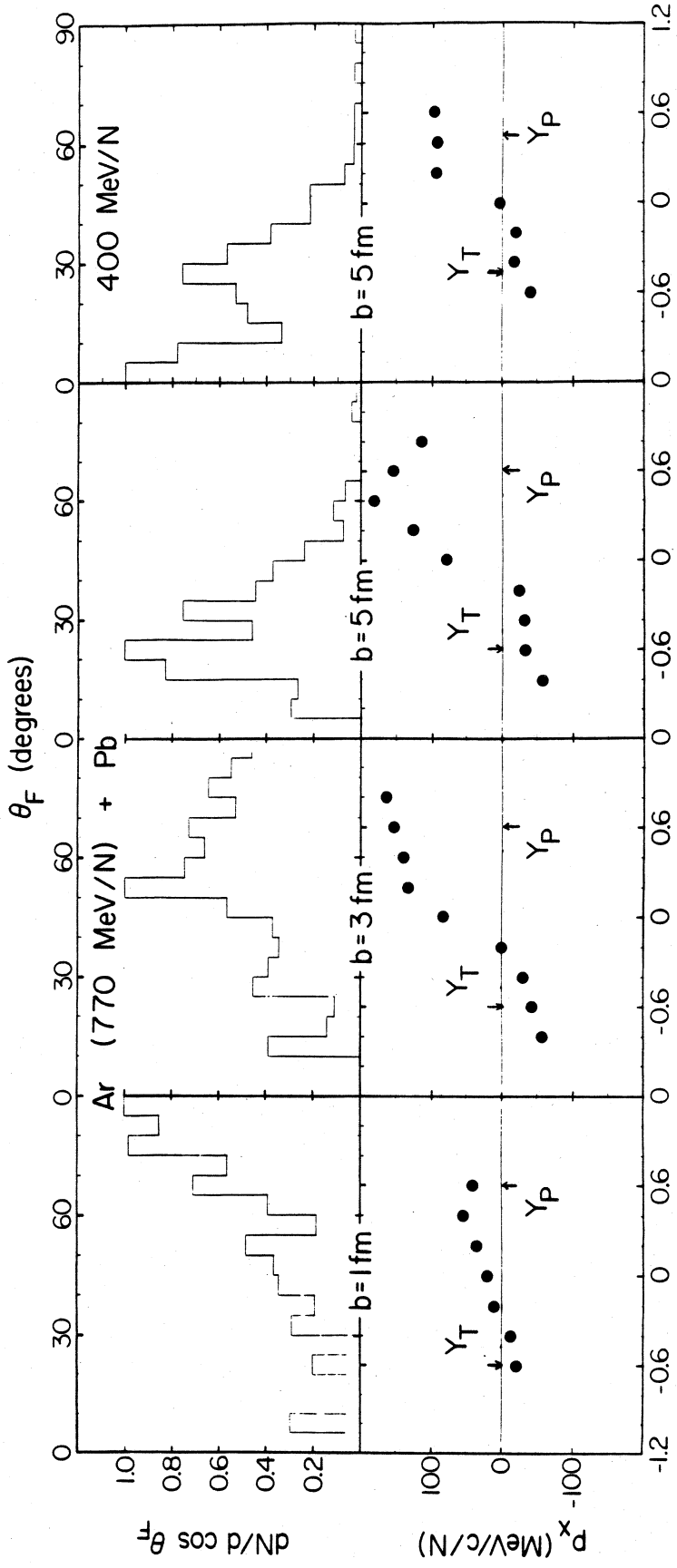

FIGURE 4

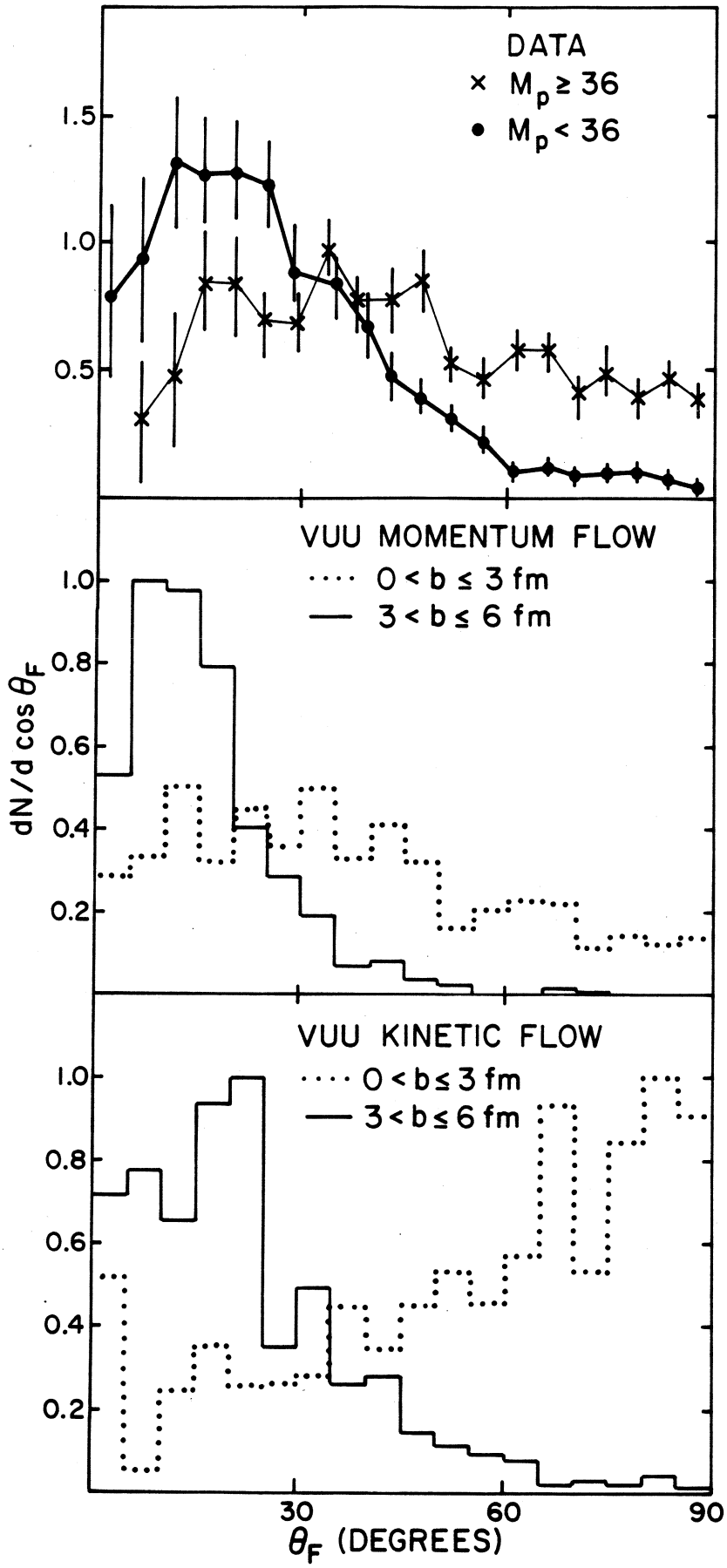
DATA
× $M_p \geq 36$
• $M_p < 36$
1.5
1.0
0.5
VUU MOMENTUM FLOW
···· $0 < b \leq 3$ fm
— $3 < b \leq 6$ fm
1.0
0.8
0.6
0.4
0.2
$dN/d\cos\theta_F$
VUU KINETIC FLOW
···· $0 < b \leq 3$ fm
— $3 < b \leq 6$ fm
1.0
0.8
0.6
0.4
0.2
30
60
90
θ_F (DEGREES)

FIGURE 5